Diamond & Related Materials 18 (2009) 452–456

Contents lists available at ScienceDirect

Diamond & Related Materials

journal homepage: www.elsevier.com/locate/diamond

Field emission properties of CNT–ZnO composite materials

Chien-Sheng Huang [a,*], Chun-Yu Yeh [a], Yung-Huang Chang [b], Yi-Min Hsieh [a], Chien-Yeh Ku [a], Quan-Ting Lai [a]

[a] Graduate school of Optoelectronics, National Yunlin University of Science and Technology, Douliou 64002, Taiwan
[b] Department of Materials Science and Engineering, National Chiao Tung University, Hsinchu 30050, Taiwan

ARTICLE INFO

Available online 12 November 2008

Keywords:
CNT–ZnO
Composite materials
Field emission properties

ABSTRACT

CNT–ZnO composite materials were successfully grown by thermal chemical vapor deposition (thermal CVD). First, Multiwalled Carbon nanotubes were synthesized in the temperature range of 500–700 °C. After coating Au nanoparticles on such grown CNTs, ZnO nanowires were synthesized via Zn evaporation method at 500 °C. SEM images showed that these CNT–ZnO composites were spinous, and XRD analyses showed that the spinal ZnO were crystalline. The turn-on field of CNT–ZnO composite materials with 500 °C growth temperature of underlying CNTs was 3.72 V/μm, which was 5.58 V/μm for CNTs grown at 500 °C. It was also found that the higher temperature (<550 °C) the underlying CNTs were grown at, the better field emission properties CNT–ZnO composite materials have. The I_D/I_G ratio from Raman spectroscopy of CNTs decreased as the growth temperature of CNTs increased. The graphitization of underlying CNTs played an important role in the Field emission of CNT–ZnO composite materials.

1. Introduction

One-dimensional (1D) nanostructural materials have attracted considerable attention due to their unique fundamental physical properties and potential high-technology applications in the fabrication of nanoscale devices [1]. The nanotubes and nanowires are promising candidates of ideal field emission electron sources because of their high aspect ratio geometry and small tip radius of curvature. Since the discovery of carbon nanotubes (CNTs) in 1991 [2], they have been the most promising material due to their unique structure and properties. ZnO, as an oxide, presents many remarkable characteristics due to its high mechanical strength, good optical quality, chemical stability and excellent piezoelectric properties [3]. In the past, many studies have investigated the field emission properties of CNTs [4–6] and ZnO nanostructures [7–10].

In this study, a CNT–ZnO composite was synthesized and exhibited different field emission properties from general CNTs or ZnO nanowires.

2. Experimental details

The growth of CNTs was carried out by using the thermal chemical vapor deposition (thermal CVD) system at temperatures of 500 °C, 550 °C, 600 °C, 650 °C, and 700 °C. Prior to the growth, an Fe layer was deposited as catalysts on a (100) p-type silicon substrate by the RF sputtering with Ar plasma. During the growth, the N_2 gas was first introduced into reaction tube at a flow rate of 100 sccm with 8.67×10^2 Pa for 30 min. Reaching the growth temperature, N_2 was switched off and C_2H_2 was switched on at a flow rate of 30 sccm with 4.67×10^2 Pa for 20 min, and then swiched off. Finally, the reaction tube was cooled down at the N_2 ambient.

Such grown CNTs was then coated Au as the catalyst to synthesize ZnO. By heating pure zinc powder at the temperature 500 °C in a horizontal tube furnace and using Argon and oxygen gases as a carrier and a reaction gas during the fabrication process, spinal ZnO was formed on the underlying carbon nanotubes.

The morphology and crystal structure properties of the samples were examined by field emission scanning electron microscopy (FE-SEM), Raman spectroscopy, and X-ray diffractometer (XRD), respectively. Field emission measurements were carried out by using a diode configuration in a vacuum chamber, which was pumped down to 2.67×10^{-4} Pa, and using a Keithley 237 source meter as an analyzer. The turn-on electric fields of tested materials were calculated from the values of voltage Vto divided by the average gap between the material surface and the anode. Vto was measured when the field emission current reached 1.0 μA, and the uncertainty was ±1 V. The gap was measured by a step gauge, and the uncertainty was ±1 μm.

3. Results and discussion

Fig. 1 showed the SEM image of underlying CNTs at growth temperatures range of 500–700 °C. It was found that the higher

* Corresponding author.
E-mail address: huangchs@yuntech.edu.tw (C.-S. Huang).

0925-9635/$ – see front matter © 2008 Elsevier B.V. All rights reserved.
doi:10.1016/j.diamond.2008.10.058

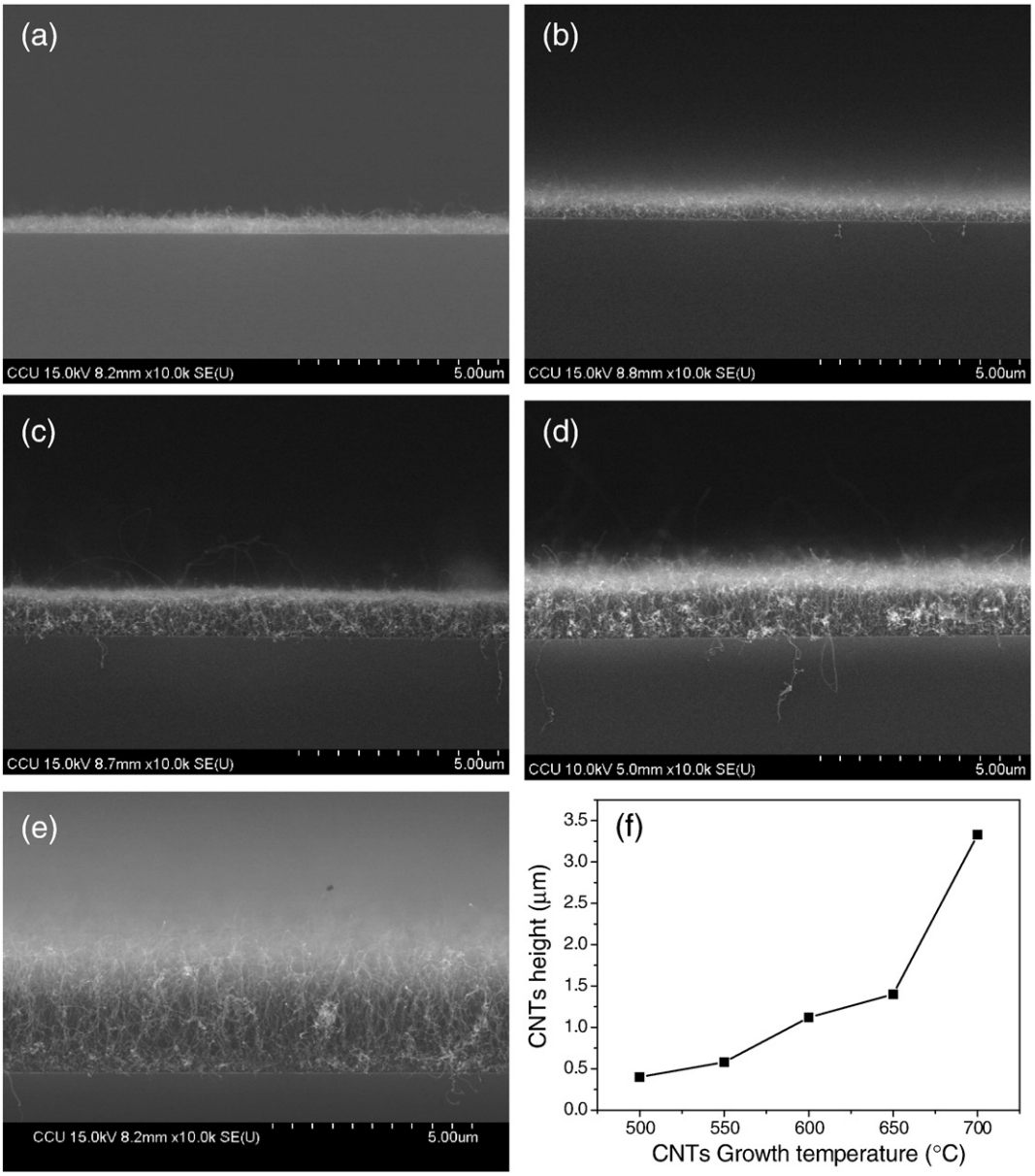

Fig. 1. SEM images of underlying CNTs at different growth temperatures: (a) 500 °C, (b) 550 °C, (c) 600 °C, (d) 650 °C, (e) 700 °C; and (f) the height of underlying CNTs versus growth temperatures.

temperature the CNTs were grown at, the height of CNTs increased from 0.58 to 3.33 μm.

Fig. 2 showed the Raman spectra (taken with the 532 nm Nd:YAG laser) of underlying CNTs at the growth temperature range of 500–700 °C. Both the typical D band (~1350 cm^{-1}) and G band (~1580 cm^{-1}) for multi-walled CNTs appeared [11]. The Lorentzian components fitting gave the peak values and the ratio I_D/I_G, which would be a graphitization index for CNTs. It was found that the higher temperature the CNTs were grown at, the I_D/I_G ratio of CNTs decreased from 1.165 to 0.800. As stated in the literatures [12–14], CNTs grown at higher temperatures would have smaller I_D/I_G ratio and therefore higher graphitic crystallinity.

Fig. 3(a) showed the SEM image of Au nanoparticles on the underlying CNTs. Au nanoparticles have the diameter of ~5 nm. Fig. 3(b)–(f) showed SEM images of the CNT–ZnO composite with the underlying CNTs of different growth temperatures. The XRD pattern of CNT–ZnO composite was shown in Fig. 4. All diffraction peaks matched the wurtzite ZnO structure with the lattice constants of a=0.325 nm and c=0.52 nm (JCPDS No. 36-1451). The peaks at which 2θ equals 31.7°, 34.4°, 36.3°, 47.5°, and 56.6° represent ZnO (100), (002), (101), (102), and (110) reflections, respectively.

The field emission (FE) properties were characterized by using a Keithley 237 source meter as an analyzer. The FE current–voltage characteristics were further analyzed by a simplified Fowler–Nordheim (F–N) equation:

$$J = \frac{A\beta^2 E^2}{\phi} \exp\left(-B\frac{\phi^{3/2}}{\beta E}\right) \quad (1)$$

where J is the emission current density, E is the macroscopic field, ϕ is the work function of the emitter, A and B are the F–N constants with values of 1.56×10^{-10} A eVV^{-2} and 6.83×10^{3} eV$^{-3/2}$V μm^{-1}, respectively [15]. The β is the FE enhancement factor that represents the true value of the electric field at the tip compared to its average macroscopic value. The β can be calculated from the slope of the FN plot [$\ln(J/E^2)$ versus $1/E$ plot] if the work function is known.

Fig. 5(a) and (b) showed the emission current density of the underlying CNTs with different growth temperatures versus electric

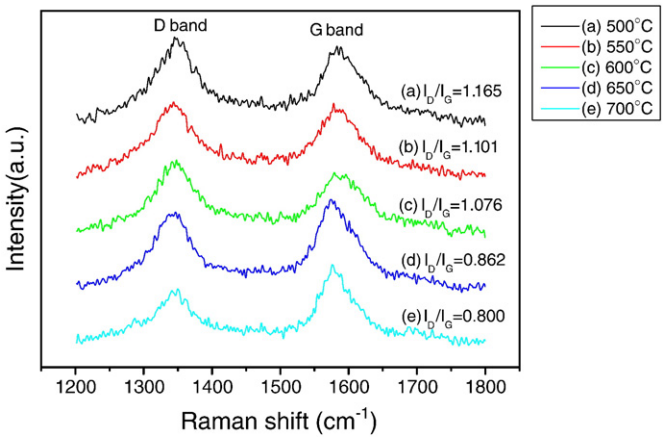

Fig. 2. Raman spectra of underlying CNTs at different growth temperatures: (a) 500 °C, (b) 550 °C, (c) 600 °C, (d) 650 °C, (e) 700 °C.

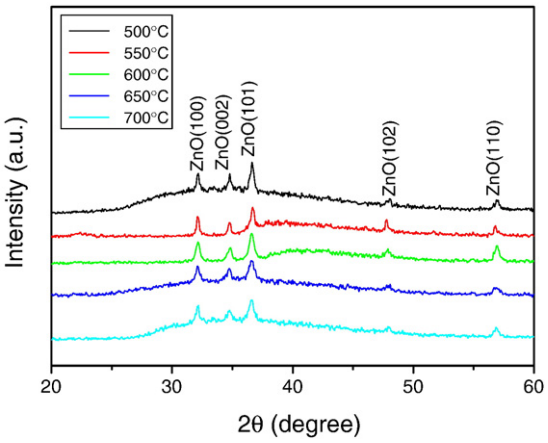

Fig. 4. XRD pattern of CNT–ZnO composite materials with different growth temperature of underlying CNTs.

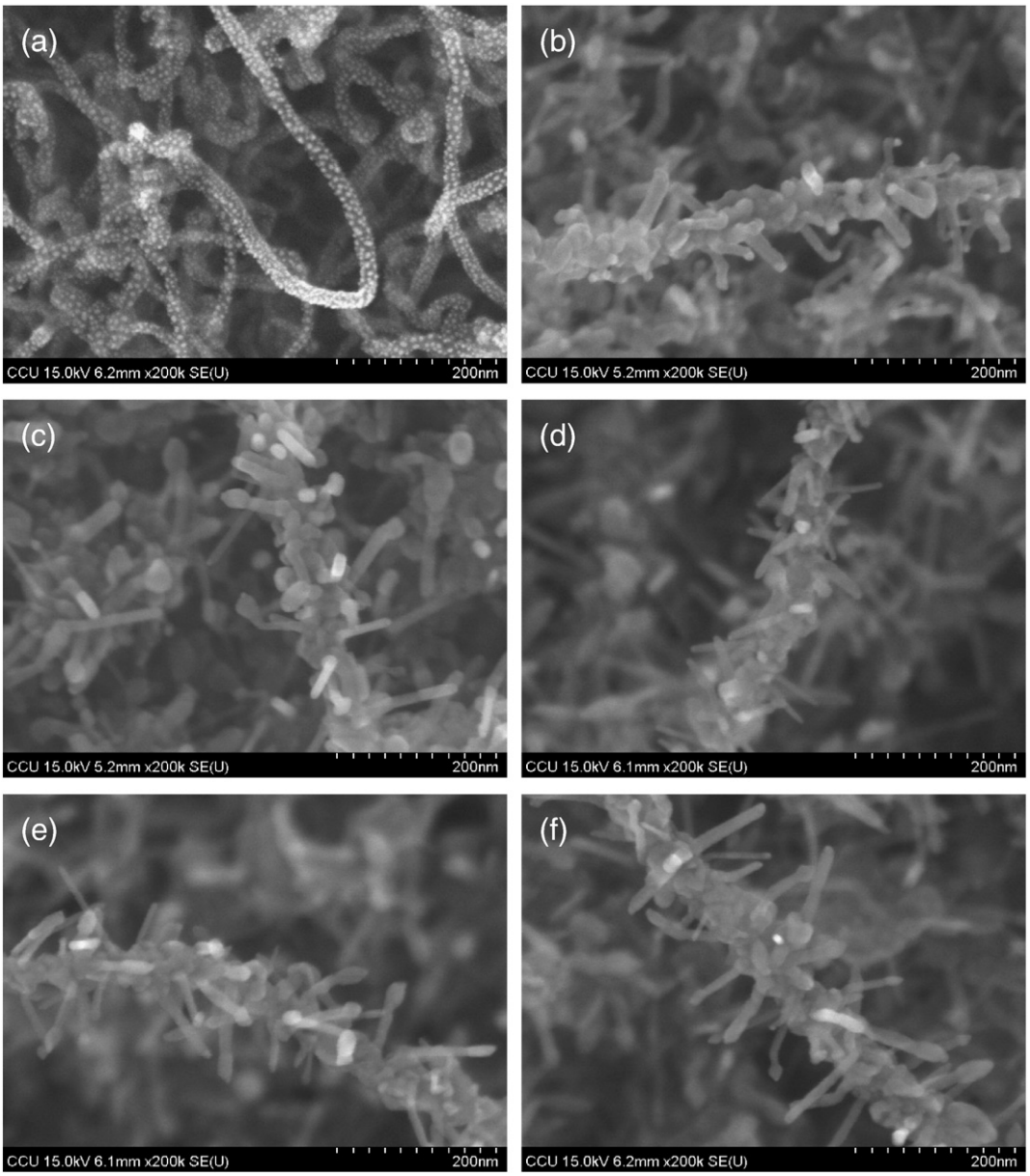

Fig. 3. SEM images of (a) Au nanoparticles on underlying CNTs and CNT–ZnO composite materials with different growth temperature of underlying CNTs: (b) 500 °C, (c) 550 °C, (d) 600 °C, (e) 650 °C, (f) 700 °C.

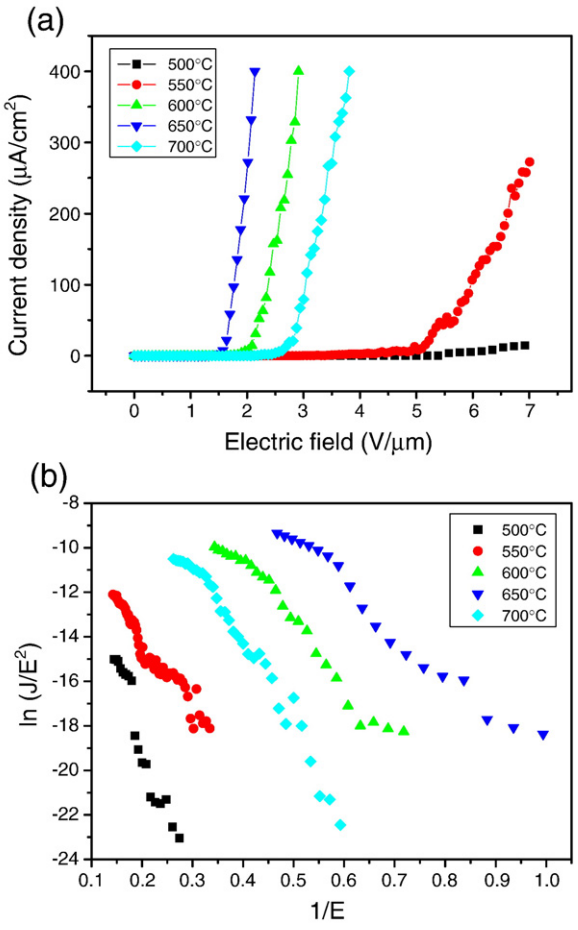

Fig. 5. (a) Emission current density versus electric field, and (b) the corresponding F–N plot of the underlying CNTs with different growth temperature.

field, and the corresponding F–N plot, respectively. The work function of CNTs was assumed to be 5 eV [16]. As the growth temperature of underlying CNTs increased from 500, 550, 600 to 650 °C, the turn-on field was decreased from 5.58, 3.50, 1.84 to 1.45 V/μm and the β was increased from 1167, 2077, 3604 to 6032, respectively. By comparison with the Raman spectroscopy in the Fig. 2, the tendency was obvious that the underlying CNTs grown at higher temperatures (≥650 °C) would have higher graphitic crystallinity, lower field emission turn-on field and larger β. This was also stated in the literature that the emission current of CNTs increased with the graphitic crystallinity and the growth temperature of CNTs [17]. However, CNTs grown at 700 °C had the turn-on field of 2.25 V/μm and the β of 3075, not better than that of which grown at 600 °C. Since the field emission properties of CNTs mat were dependant not only on the single nanotube, but also the field-screening effect caused by the proximity of neighboring nanotubes [18], such emission property degradation of CNTs grown at 700 °C could be explained.

As stated in the literature [19], when the height of CNTs was deucedly high, the field-emission characteristic was poor, which was likely to be due to the screening effect. As the underlying CNTs grown at higher temperatures (≥600 °C), the heights were order of micro-meter magnitude. The reason was that the CNT–ZnO composites with higher temperatures CNTs (≥600 °C) were affected by field-screening effect. Because the height of CNTs at 700 °C was extremely greater than that others, its field-screening effect was especially enormous, and degraded the turn-on field and the FE enhancement factor β.

The general ZnO nanowires were synthesized on silicon (100) substrates with Au catalysts by heating pure zinc powder at temperatures 500 °C in a horizontal tube furnace. Fig. 6(a) showed SEM image of general ZnO nanowires with diameters of 80–100 nm, and Fig. 6(b) with the inset showed the emission current density versus electric field and the corresponding F–N plot of ZnO nanowires. The turn-on field was 4.90 V/μm. Assuming the work function of ZnO was 5.3 eV [20], the β was estimated to be 1225.

Fig. 7(a) and (b) showed emission current density of CNT–ZnO composite materials versus electric field, and the corresponding F–N plot, respectively. Each curve represented a CNT–ZnO composite with the underlying CNTs grown at different temperatures of 500–700 °C. The work function of CNT–ZnO composite materials was estimated to be 5.15 eV, an average value between 5 and 5.3 eV, and to calculate the field enhancement factor β [21]. For the CNT–ZnO composites, as the growth temperatures of underlying CNTs increased from 500, 550, 600, 650 to 700 °C, the turn-on fields were 3.72, 2.68, 2.40, 1.64 and 2.68 V/μm, respectively. And the β's were 2082, 2442, 2576, 4490 and 2426, respectively. All the CNT–ZnO composite materials have better field emission ability than that of general ZnO nanowires. However, by comparison with CNTs mat, the field emission properties of CNT–ZnO composites could be categorized as two groups: one is with lower turn-on voltage and higher β than that of corresponding CNTs mat grown at the same temperature (500 °C, 550 °C), and the other is with higher turn-on voltage and lower β than that of corresponding CNTs mat grown at the same temperature (600 °C, 650 °C, 700 °C). From Fig. 1(f), the height of underlying CNTs of the former group was about hundreds of nano-meter magnitude, and the one of the latter group was above the order of micro-meter magnitude. As mentioned, the

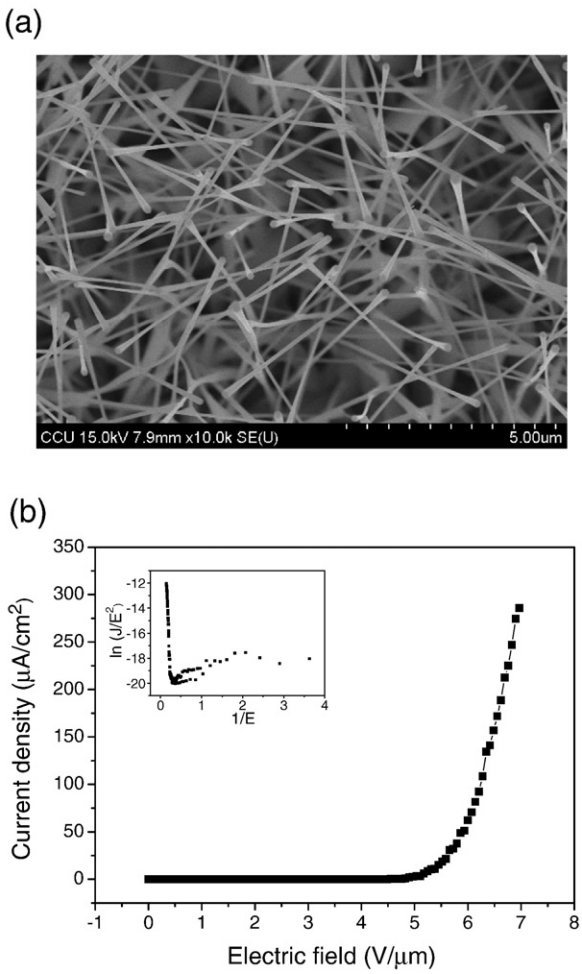

Fig. 6. (a) SEM images, and (b) Emission current density versus electric field of ZnO nanowires with diameters of 80–100 nm.

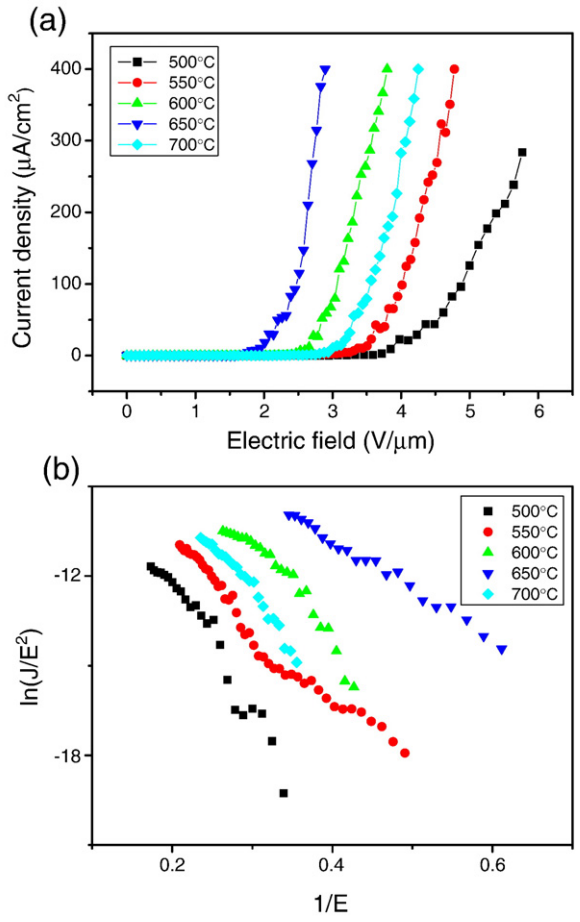

Fig. 7. (a) Emission current density versus electric field, and (b) the corresponding F–N plot of CNT–ZnO composite materials with different growth temperature of underlying CNTs.

screening effect was important when the height of CNTs were deucedly high. The field emission experiments of CNT–ZnO composites showed that micro meter seemed to be a criterion scale. Hence the field emission properties of CNT–ZnO composites, which had the underlying CNTs grown at 500 and 550 °C, were better than that of general CNTs grown at the same temperature. The reason was that the spinal ZnO on the surface of CNT–ZnO composite played as a sharp emission center.

4. Conclusions

The field-emission characteristics of CNT–ZnO composite were different from that of general CNTs or ZnO nanotubes, and the temperature at which the underlying CNTs were grown exhibited great effects on it. The turn-on field of CNT–ZnO composite materials with 500 °C and 550 °C growth temperature of underlying CNTs were 3.72 and 2.68 V/μm, which were 5.58 and 3.50 V/μm for CNTs grown at 500 °C and 550 °C, respectively. The spinal ZnO on the surface of CNT–ZnO composites played as a sharp emission center and gave rise to the increasing of β factor. However, the screening effect should be considered when the height of CNTs increased to a few micro-meter scale ranges.

References

[1] Y. Xia, P. Yang, Y. Sun, Y. Wu, B. Mayers, B. Gates, Y. Yin, F. Kim, H. Yan, Adv. Mater. (Weinheim, Ger.) 15 (2003) 353.
[2] S. Iijima, Nature 354 (1991) 56.
[3] S.J. Pearton, D.P. Norton, K. Ip, Y.W. Heo, T. Steiner, Superlattice Microstruct. 34 (2003) 3.
[4] W.A. de Heer, A. Chatelain, D. Ugarte, Science 270 (1995) 1179.
[5] S.C. Tseng, C.H. Li, Y.Y. Lin, Ching Hsiang Tsai, Z.P. Wang, K.C. Leou, C.H. Tsai, S.P. Chen, J.Y. Lee, B.C. Yao, Diamond Relat. Mater. 14 (2005) 2064.
[6] Y.M. Wong, W.P. Kang, J.L. Davidson, B.K. Choi, W. Hofmeister, J.H. Huang, Diamond Relat. Mater. 14 (2005) 2069.
[7] W.I. Park, D.H. Kim, S.-W. Jung, G.-C. Yi, Appl. Phys. Lett. 80 (2002) 4232.
[8] C.J. Lee, T.J. Lee, S.C. Lyu, Y. Zhang, H. Ruh, H.J. Lee, Appl. Phys. Lett. 81 (2002) 3648.
[9] M.H. Huang, S. Mao, H. Feich, H. Yan, Y. Wu, H. Kind, E. Weber, R. Russo, P. Yang, Science 292 (2001) 1897.
[10] C.X. Xu, X.W. Sun, B.J. Chen, Appl. Phys. Lett. 84 (2004) 1540.
[11] M.S. Dresselhaus, G. Dresselhaus, P.H. Avouris, Carbon Nanotubes: Synthesis, Properties and Applications, Springer Series in Topics in Applied Physics, vol. 80, Springer-Verlag, Berlin, 2001.
[12] P.H. Tan, S.L. Zhang, K.T. Yue, F.M. Huang, Z.J. Shi, X.H. Zhou, Z.N. Gu, J. Raman Spectrosc. 28 (5) (1997) 369.
[13] C.F. Chen, C.L. Tsai, C.L. Lin, Diamond Relat. Mater. 12 (2003) 1500.
[14] L. Valentini, I. Armentano, J.M. Kenny, L. Lozzi, S. Santucci, Diamond Relat. Mater. 12 (2003) 821.
[15] R.H. Fowler, L. Nordheim, Proc. R. Soc. London, Ser. A 119 (1928) 173.
[16] J.M. Bonard, J.P. Salvetat, T. Stockli, L. Forro, A. Chatelain, Appl. Phys. A: Mater. Sci. Process. 69 (1999) 245.
[17] L. Wang, Z. Sun, T. Chen, W. Que, Solid-State Electron. 50 (2006) 800.
[18] L. Nilsson, O. Groening, C. Emmenegger, O. Kuettel, E. Schaller, L. Schlapbach, H. Kind, J-M. Bonard, K. Kern, Appl. Phys. Lett. 76 (2000) 2071.
[19] S. Fujii, S. Honda, H. Kawai, K. Ishida, K. Oura, M. Katayama, Diamond Relat. Mater. 17 (2008) 556.
[20] C.J. Lee, T.J. Lee, S.C. Lyu, Y. Zhang, H. Ruh, H.J. Lee, Appl. Phys. Lett. 81 (2002) 3648.
[21] J.M. Green, L. Dong, T. Gutu, J. Jiao, J.F. Conley Jr., Y. Ono, J. Appl. Phys. 99 (2006) 094308.